

Potential barrier increase due to Gd doping of BiFeO₃ layers in Nb:SrTiO₃-BiFeO₃-Pt structures displaying diode-like behavior

H. Khassaf, G. A. Ibanescu, I. Pintilie, I. B. Misirlioglu, and L. Pintilie

Citation: *Appl. Phys. Lett.* **100**, 252903 (2012); doi: 10.1063/1.4729816

View online: <http://dx.doi.org/10.1063/1.4729816>

View Table of Contents: <http://apl.aip.org/resource/1/APPLAB/v100/i25>

Published by the [American Institute of Physics](#).

Related Articles

Influences of leakage currents on the transport properties and photoelectric effects in heterojunctions composed of colossal magnetoresistance manganites and Nb-doped titanates

J. Appl. Phys. **111**, 07D724 (2012)

Rectifying characteristics, magnetic tunability, and photovoltaic response in La_{0.8}Hf_{0.2}MnO₃/0.7 wt% Nb-SrTiO₃ heteroepitaxial junctions

J. Appl. Phys. **111**, 07D723 (2012)

Rectifying behaviors induced by BN-doping in trigonal graphene with zigzag edges

Appl. Phys. Lett. **100**, 063107 (2012)

Three-dimensional shaping of sub-micron GaAs Schottky junctions for zero-bias terahertz rectification

Appl. Phys. Lett. **99**, 263505 (2011)

Rectifying characteristic of perovskite oxide La_{1.89}Ce_{0.11}CuO₄/Ba_{0.5}Sr_{0.5}TiO₃/La_{0.67}Sr_{0.33}MnO₃ heterostructures

J. Appl. Phys. **110**, 103716 (2011)

Additional information on *Appl. Phys. Lett.*

Journal Homepage: <http://apl.aip.org/>

Journal Information: http://apl.aip.org/about/about_the_journal

Top downloads: http://apl.aip.org/features/most_downloaded

Information for Authors: <http://apl.aip.org/authors>

ADVERTISEMENT



Agilent Technologies

Agilent Education and Research Resources DVD 2012

Packed with over **100 NEW** articles, application notes, webcasts, and videos relating to Renewable Energy, Nanoscience, RF/Wireless, MIMO, Materials, Digital Signals, Photonics, and General Test & Measurement.

Click Here to
Order Your DVD



Agilent Technologies

Potential barrier increase due to Gd doping of BiFeO₃ layers in Nb:SrTiO₃-BiFeO₃-Pt structures displaying diode-like behavior

H. Khassaf,¹ G. A. Ibanescu,² I. Pintilie,² I. B. Misirliloglu,¹ and L. Pintilie²

¹Faculty of Engineering and Natural Sciences, Sabanci University, Orhanli-Tuzla, 34956 Istanbul, Turkey

²National Institute of Materials Physics, Atomistilor 105bis, Magurele 077125, Romania

(Received 12 April 2012; accepted 26 May 2012; published online 19 June 2012)

The rectifying properties of Nb:SrTiO₃-Bi_{1-x}Gd_xFeO₃-Pt structures ($x = 0, 0.05, 0.1$) displaying diode-like behavior were investigated via current-voltage characteristics at different temperatures. The potential barrier was estimated for negative polarity assuming a Schottky-like thermionic emission with injection controlled by the interface and the drift controlled by the bulk. The height of the potential barrier at the Nb:SrTiO₃-Bi_{1-x}Gd_xFeO₃ interface increases with Gd doping. The results are explained by the partial compensation of the p -type conduction due to Bi vacancies with Gd doping in addition to the shift of the Fermi level towards the middle of the bandgap with increasing dopant concentration. © 2012 American Institute of Physics. [<http://dx.doi.org/10.1063/1.4729816>]

Owing to its multiferroic behavior at room temperature (RT), BiFeO₃ (BFO) has attracted a considerable interest for application in microelectronics, especially for non-volatile memories.¹⁻⁸ It has also been considered as a candidate to replace lead-based piezoelectric ceramics.^{9,10} One major problem hindering the applications based on BFO thin films is the presence of high leakage currents that screen the applied field and obscure the current peaks associated with polarization (P) reversal in this system.¹¹⁻¹⁴ Among the methods to reduce leakage was doping with iso- or heterovalent atoms replacing Bi or Fe in the BFO lattice, such as La, Nb, Ca, Mn, Cr, Gd, or alloying with other perovskites.¹⁵⁻²¹ Particularly, Gd is of interest due to the fact that, owing to its high valence spin state, it may induce some ferromagnetic activity which is more attractive for applications compared to the antiferromagnetism specific for pure BFO. Reduction in leakage was reported for Gd doped BFO films deposited by metal organic decomposition on platinized Si wafers.²² Another work reported that the leakage current in epitaxial BFO layers deposited by pulsed laser deposition (PLD) on single crystal SrTiO₃ substrates with SrRuO₃ electrodes can be manipulated via control of the orientation of the BFO layer.²³ BFO deposited directly on Nb doped conducting SrTiO₃ single crystal substrates (Nb:SrTiO₃, shortly STON) with Pt top electrode also leads to a structure with diode-like behavior.²⁴ Despite the very recent interest in such structures, there is no systematic study reporting on the height of the potential barrier at the STON-BFO interface as well as the dopant dependence of the potential barrier.

In the present study we report on control of the barrier height by Gd doping of the BFO layer in a Nb:SrTiO₃-Bi_(1-x)Gd_xFeO₃-Pt (STON-BFGO-Pt) structure with [001] direction of STON perpendicular to the plane ($x = 0, 0.05, 0.1$). The BFGO layer was prepared by sol-gel deposition on (001) STON substrates having 0.7% Nb doping. X-ray diffraction analysis showed that the pure and doped BFO layers grow quasi-epitaxially (columnar) on single crystal substrates at a thickness of around 100 nm with the (001) and (002) film peaks visible while other bulk BFO peaks are absent (Fig. 1(a)). The top Pt contacts of $0.1 \times 0.1 \text{ mm}^2$ were

deposited by magnetron RF-sputtering through a shadow mask. The electric measurements were performed at different temperatures in a cryogenic probe station from Lake-Shore (model CPX-VF). The capacitance of the samples were measured with a Hioki LRC bridge, the leakage current with a Keithley 6517 electrometer and the hysteresis loop with a TF2000 ferroelectric tester from AixAcct.

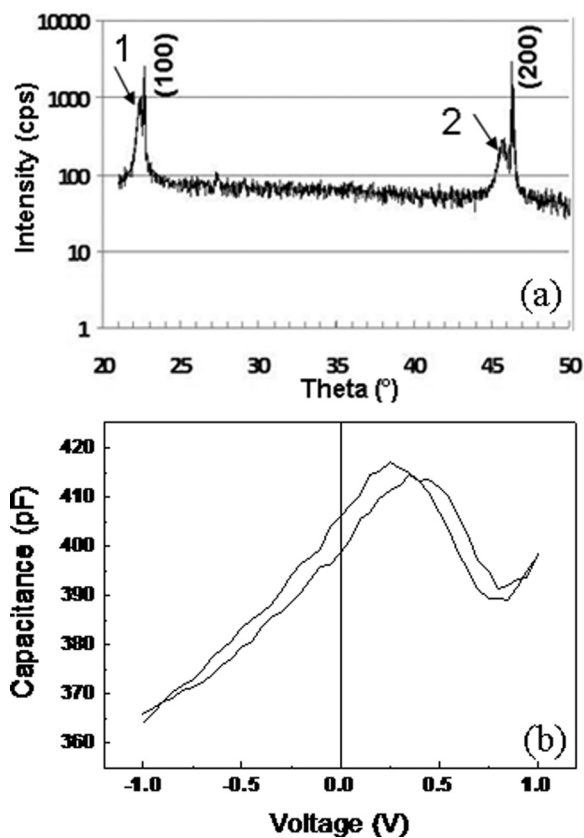


FIG. 1. (a) XRD pattern of the pure BFO film where 1 and 2 denote the (100) and (200) peaks of the film, respectively. Note that Gd doped films have nearly the same pattern (not shown here), (b) C-V characteristic at RT for single phase BFO layer. Measurement performed at 100 kHz with an amplitude of 0.1 V for the ac signal.

Polarization-applied field (P - E) measurements showed that the hysteresis loops both in pure and doped BFO were severely distorted by the leakage current even at temperatures lower than RT. The ferroelectric behavior of the BFO layers could be confirmed only by capacitance-voltage (C - V) characteristics as shown in Fig. 1(b) where butterfly shape specific for ferroelectrics is observed. The shift between the sweep-up and sweep-down characteristics is small, suggesting a small coercive field. Moreover, the fact that the switching takes place only in one polarity indicates the presence of a considerable internal electric field, probably due to highly asymmetric charge accumulations at each interface,²⁵ similar to the one reported recently for SrRuO₃-Pb(Zr,Ti)O₃-Ta Schottky like diodes.²⁶ It has to be noted that the sample does not behave as an ideal ferroelectric capacitor, where the voltage dependence of the capacitance is given only by the reversal of P . The C - V curve has to correlate with the current-voltage (I - V) characteristics at RT, which are presented in the Fig. 2 for pure and doped BFO. The asymmetry shows that the STON-BFO-Pt structure has a diode like behavior, being forward biased for positive voltages applied on the top Pt contact and reverse biased for negative voltages applied on Pt. The current magnitude does not vary much with the Gd doping and rectification ratio is not very high, being around 40 at ± 1 V. Returning to the C - V characteristic shown in Fig. 1(b), the peculiar voltage dependence on the positive polarity may be related to the voltage dependent space charges which are present in the diode like structure.

In order to gain further insight, the I - V characteristics at different temperatures were performed on pure and doped BFO layers. The results are given in Fig. 3. It is clear that, for the negative polarity there is a great temperature dependence of the leakage current, about 2 orders of magnitude or more at a voltage of -1 V. On the positive polarity side, the temperature dependence is more evident at low voltages, below 0.6 V. At higher voltages the temperature dependence diminishes, and the steps occurring in the I - V characteristics at certain voltages support the hypothesis that the leakage current for forward bias at high voltages is dominated by space charge limited currents (SCLC) possibly with an exponential distribution of traps.²⁷ It has to be noted that the transition to SCLC happens in the same voltage domain where the C - V characteristic shows the peculiar voltage depend-

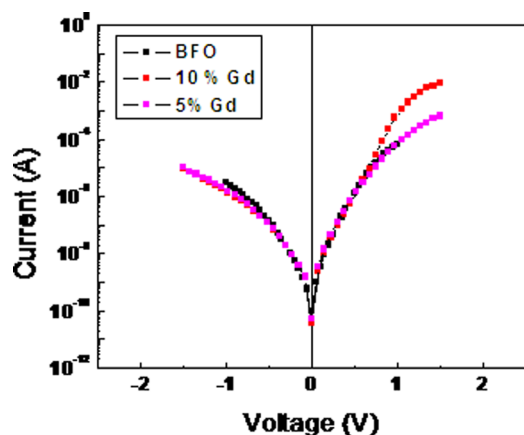


FIG. 2. I - V characteristics at RT for different Gd doping of the BFO layer.

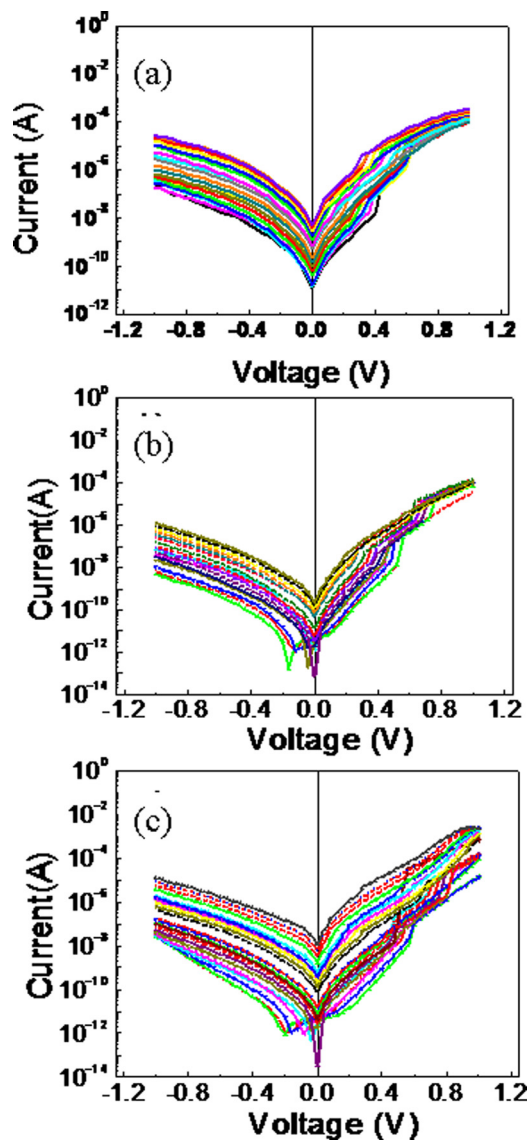


FIG. 3. I - V characteristics at different temperatures for BFO films with no Gd doping (a), with 5% Gd doping (b) and with 10% Gd doping (c).

ence. It can be assumed that the redistribution of space charges makes the voltage dependence of the capacitance more complicated for the present diode-like structure compared to the ideal ferroelectric capacitors.

In the following paragraphs, only the negative part of the I - V characteristics will be analyzed in detail. The rectifying behavior of the STON-BFO-Pt structure suggests that thermionic emission over a potential barrier may be responsible for the leakage current in reverse bias. The question is the following: Is the potential barrier located at the STON-BFO interface or at the BFO-Pt interface? It could be that potential barriers exist at both interfaces but one of them is lower, leading to the diode-like I - V behavior. Another unknown is the conduction type of BFO in bulk of the film. Previous reports suggest p -type conduction due to Bi losses during PLD deposition or during crystallization annealing in the case of sol-gel deposited films.^{24,28} Work of Guo *et al.* on a similar pseudocubic perovskite (LiNbO₃) shows that LiNbO₃ exhibits a p -type conductivity due to Li losses during fabrication.²⁹ Assuming that the BFO films in the present study are also p -type, the reverse bias occurs when negative

voltage is applied on the top Pt electrode, meaning positive polarity on the bottom STON substrate. Therefore, it can be concluded that the reverse biased Schottky contact is located at the bottom STON-BFO interface while the top BFO-Pt interface behaves as a quasi-ohmic contact.

With the above proposition in mind, the temperature dependence of the negative part of the I-V characteristics in Fig. 3 was analyzed considering a conduction mechanism in which the injection of charge is controlled by the potential barrier existing at the STON-BFO interface while the drift in the ferroelectric film is controlled by the bulk. The Schottky-Simmons equation was used³⁰

$$J = 2q \left(\frac{2\pi m_{eff} kT}{h^2} \right)^{3/2} \mu E \exp \left(-\frac{q}{kT} \left(\Phi_B^0 - \sqrt{\frac{qE_m}{4\pi\epsilon_0\epsilon_{op}}} \right) \right). \quad (1)$$

Here q is the electron charge, h is the Planck's constant, m_{eff} is the effective mass, k is the Boltzmann's constant, μ is the mobility of electrons in the conduction band of BFO, E is the electric field in the bulk of BFO, T is the temperature, Φ_B^0 is the potential barrier at zero bias, E_m is the maximum field at the interface if a Schottky-like contact is present (depletion region width is voltage dependent), ϵ_0 is the vacuum permittivity, and ϵ_{op} is the dielectric constant at optical frequencies. E_m is given by³¹

$$E_m = \sqrt{\frac{2qN_{eff}(V + V_{bi})}{\epsilon_0\epsilon_{st}}} + \frac{P}{\epsilon_0\epsilon_{st}}. \quad (2)$$

Here N_{eff} is the effective density of charge in the depleted region of the Schottky type contact, P is the ferroelectric polarization, V_{bi} is the built-in potential (including the contribution of ferroelectric polarization), and ϵ_{st} is the static dielectric constant. The voltage dependence of J in Eq. (1) will be dictated by the dominant term in Eq. (2). If the polarization term is dominant ($\sqrt{2qN_{eff}(V + V_{bi})/\epsilon_0\epsilon_{st}} \ll P/\epsilon_0\epsilon_{st}$) then $\log J \propto V^{1/2}$ and Φ_B^0 is drastically reduced by P . If the P term is negligible in Eq. (2) then $\log J \propto V^{1/4}$. It must be noted that Eq. (2) applies if the ferroelectric film is only partially depleted in the voltage range employed for electrical measurements. Referring to the samples studied in this work, it is clear that pure and doped BFO layers are partially depleted in the voltage range used for C-V measurements (see Fig. 1(b)) as the capacitance varies continuously with the applied voltage. In the case of a fully depleted film the capacitance should converge towards a constant value with increasing the voltage, which is definitely not the case. Moreover, considering the difficulty to record a P - E loop and small voltage difference between the maxima of the sweep-up and sweep-down curves in C-V measurements, it can be assumed that remnant polarization is small in the BFO layer and that the P term in Eq. (2) is negligible. Another contribution comes from the possibly large value of ϵ_{st} in our films with columnar texture. N_{eff} may be also larger than in fully epitaxial films. Thus, it is reasonable to consider the case $\log J \sim V^{1/4}$. The data were analyzed in the following way: the $\log(J/T^{3/2})$ was plotted as a function of $1000/T$

(Arrhenius plot) for a certain applied voltage, and from the slope the potential barrier at the relevant bias voltage was estimated (including the Schottky effect); the potential barriers at several applied voltages were then plotted as a function of $V^{1/4}$, and the potential barrier at zero volt was estimated from the intercept at the origin. Here, the better the linear fit the more accurate is the estimate of Φ_B^0 . However, an error up to 0.1 eV is possible while applying this method. The $V^{1/4}$ dependence of the potential barrier is presented in Fig. 4 for the BFO samples with different Gd content.

The intercept at the origin yields the following values for the potential barrier at zero volt: 0.32 eV at zero doping; 0.45 eV for 5% Gd doping; 0.60 eV for 10% Gd doping. The results show that the height of the potential barrier increases with Gd content in the BFO film. This is a very interesting result which can be explained assuming a compensation mechanism of the holes, introduced by the presence of Bi vacancies, by the electrons introduced via Gd doping. In the undoped BFO films the conduction is predominantly p -type, the Fermi level is closer to the valance band, thus the potential barrier for holes is not very high. Gd doping can compensate the p -type conduction, thus the Fermi level moves towards the middle of the forbidden band leading to an increase of the potential barrier for holes. Despite the significant increase of the potential barrier, the magnitude of the leakage current on the negative side of the I-V characteristics does not vary significantly with the Gd doping. Referring to Eq. (1) it can be seen that a quantity which may impact significantly the apparent potential barrier and the carrier injection into the ferroelectric layer is E_m . There are several quantities which can vary with the Gd content, such as N_{eff} , P , V_{bi} , and ϵ_{st} , making it hard to decide which of these quantities is contributing the most to the partial compensation of the increased barrier height.

Some useful information can be extracted from the C-V characteristics, assuming that the BFO film behaves as a wide bandgap semiconductor. The $1/C^2$ - V representation can be used to extract information about the density of the free carriers. Figure 5 shows the above representation for the case of pure BFO film. Similar results were obtained for the films doped with 5% and 10% Gd. In Fig. 5 one has to notice that the intercept at origin on the voltage axis, giving V_{bi} , is not the

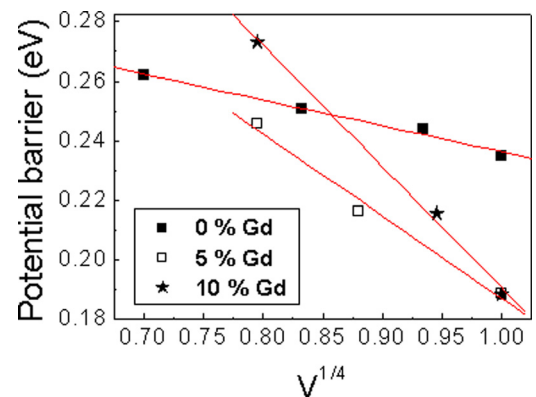


FIG. 4. The voltage dependence of the potential barrier in the case of BFO films with different Gd doping, on STON substrates. The confidence factor for the linear fit is in all cases higher than 0.99.

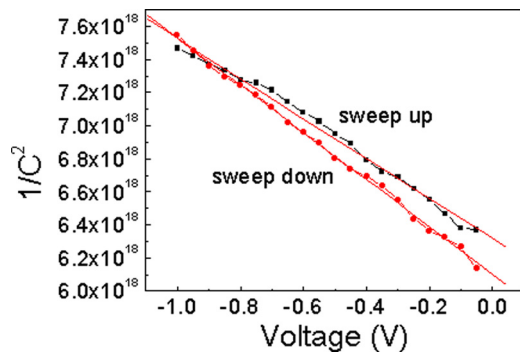


FIG. 5. The $1/C^2$ vs. voltage representation for the pure BFO film.

same for sweep up and sweep down. This fact is a finger print for the presence of the ferroelectric polarization, which is changing the band-bending at the interface depending on the sign of the polarization charge.³¹ The slope of the $1/C^2 \sim V$ dependence was used to estimate the density of the free carriers n , and the intercept was used to extract V_{bi} . The results are presented in Table I. One can see that the density of the free carriers is slightly decreasing with increasing Gd doping, supporting the hypothesis of the compensation of the p -type conduction via n -type doping. However, N_{eff} is not the same with n , as N_{eff} accounts for the total density of the fixed charge in the depletion region of the Schottky contact. N_{eff} can be larger than n because it accounts for both ionized impurities and the trapped charges in the depleted region. The difference in n for sweep up and sweep down can give an estimate for $2P$, considering that this is the charge compensating P . The obtained value for $2P$ is between 6 and 11 $\mu\text{C}/\text{cm}^2$, confirming that the “measurable” P is very low because of the screening produced by the high density of free carriers.

In conclusion it was shown that the potential barrier at the STON-BFO interface increases with Gd doping. While the concentration of the free carriers in the BFO layer decreases, the leakage current remains still too large to record a hysteresis loop. This is because the increase of the barrier height and of the built-in potential has opposite effects on the current density according to the Eqs. (1) and (2). Further studies are needed to fully elucidate the origin of the high conductivity in pure BFO films. Only in this way the compensation mechanism by doping can be effective in the reduction of the leakage current.

TABLE I. The estimated values for the density of free carriers n and for the built-in potential V_{bi} for different values of the Gd doping. The estimates were performed considering a thickness of about 100 nm for the BFO films and a value of 800 for the static dielectric constant. The last value is based on the fact that the capacitance value at -1V is about the same for all samples.

Gd doping	0%		5%		10%	
	n (cm^{-3})	V_{bi} (V)	n (cm^{-3})	V_{bi} (V)	n (cm^{-3})	V_{bi} (V)
Sweep up	1.44×10^{19}	0.26	1.43×10^{19}	0.4	1.13×10^{19}	0.46
Sweep down	1.23×10^{19}	0.06	1.08×10^{19}	0.015	8.9×10^{18}	0.026

H.K. and I.B.M. acknowledge the funding provided by TUBITAK through grant (No. 109M686). I.B.M. also acknowledges the support provided by the Turkish Academy of Sciences-GEBIP program. G.A.I., I.P., and L.P. acknowledge the financial support of the CORE program PN09-45, funded by NASR-Romania.

- ¹G. Catalan and J. F. Scott, *Adv. Mater.* **21**, 2463 (2009).
- ²J. F. Scott, *Nat. Mater.* **6**, 256 (2007).
- ³W. Eerenstein, N. D. Mathur, and J. F. Scott, *Nature* **442**, 759 (2006).
- ⁴R. Ramesh and N. A. Spaldin, *Nat. Mater.* **6**, 21 (2007).
- ⁵J. Wang, J. B. Neaton, H. Zheng, V. Nagarajan, S. B. Ogale, B. Liu, D. Viehland, V. Vaithyanathan, D. G. Schlom, U. V. Waghmare, N. A. Spaldin, K. M. Rabe, M. Wuttig, and R. Ramesh, *Science* **299**, 1719 (2003).
- ⁶T. Zhao, A. Scholl, F. Zavaliche, K. Lee, M. Barry, A. Doran, M. P. Cruz, Y. H. Chu, C. Ederer, N. A. Spaldin, R. R. Das, D. M. Kim, S. H. Baek, C. B. Eom, and R. Ramesh, *Nat. Mater.* **5**, 823 (2006).
- ⁷X. Qi, J. Dho, M. Blamire, Q. Jia, J. S. Lee, S. Foltyn, and J. L. MacManus-Driscoll, *J. Magn. Magn. Mater.* **283**, 415 (2004).
- ⁸Y. H. Chu, L. W. Martin, M. B. Holcomb, and R. Ramesh, *Mater. Today* **10**, 16 (2007).
- ⁹R. J. Zeches, M. D. Rossell, J. X. Zhang, A. J. Hatt, Q. He, C.-H. Yang, A. Kumar, C. H. Wang, A. Melville, C. Adamo, G. Sheng, Y.-H. Chu, J. F. Ihlefeld, R. Erni, C. Ederer, V. Gopalan, L. Q. Chen, D. G. Schlom, N. A. Spaldin, L. W. Martin, and R. Ramesh, *Science* **326**, 977 (2009).
- ¹⁰S. Fujino, M. Murakami, V. Anbusathaiah, S.-H. Lim, V. Nagarajan, C. J. Fennie, M. Wuttig, L. Salamanca-Riba, and I. Takeuchi, *Appl. Phys. Lett.* **92**, 202904 (2008).
- ¹¹J. Seidel, L. W. Martin, Q. He, Q. Zhan, Y.-H. Chu, A. Rother, M. E. Hawkrige, P. Maksymovych, P. Yu, M. Gajek, N. Balke, S. V. Kalinin, S. Gemming, F. Wang, G. Catalan, J. F. Scott, N. A. Spaldin, J. Orenstein, and R. Ramesh, *Nat. Mater.* **8**, 229 (2009).
- ¹²Y. P. Wang, L. Zhou, M. F. Zhang, X. Y. Chen, J. M. Liu, and Z. G. Liu, *Appl. Phys. Lett.* **84**, 1731 (2004).
- ¹³S. K. Singh and H. Ishiura, *Jpn. J. Appl. Phys.* **44**, L734 (2005).
- ¹⁴D. Lebeugle, D. Colson, A. Forget, and M. Viret, *Appl. Phys. Lett.* **91**, 022907 (2007).
- ¹⁵A. Z. Simoes, E. C. Aguiar, A. H. M. Gonzalez, J. Andres, E. Longo, and J. A. Varela, *J. Appl. Phys.* **104**, 104115 (2008).
- ¹⁶Z. X. Cheng, X. L. Wang, Y. Du, and S. X. Dou, *J. Phys. D: Appl. Phys.* **43**, 242001 (2010).
- ¹⁷Y. H. Lin, Q. Jiang, Y. Wang, C. W. Nan, L. Chen, and J. Yu, *Appl. Phys. Lett.* **90**, 172507 (2007).
- ¹⁸A. Z. Simoes, F. G. Garcia, and C. S. Riccardi, *J. Alloys. Compd.* **493**, 158 (2010).
- ¹⁹Q. H. Jiang, C. W. Nan, and Z. J. Shen, *J. Am. Ceram. Soc.* **89**, 2123 (2006).
- ²⁰V. R. Palkar, D. C. Kundaliya, S. K. Malik, and S. Bhattacharya, *Phys. Rev. B* **69**, 212102 (2004).
- ²¹M. A. Khan, T. P. Comyn, and A. J. Bell, *Appl. Phys. Lett.* **92**, 072908 (2008).
- ²²G. D. Hu, X. Cheng, W. B. Wu, and C. H. Yang, *Appl. Phys. Lett.* **91**, 232909 (2007).
- ²³L. Pintilie, C. Dragoi, Y. H. Chu, L. W. Martin, R. Ramesh, and M. Alexe, *Appl. Phys. Lett.* **94**, 232902 (2009).
- ²⁴H. Yang, H. M. Luo, H. Wang, I. O. Usov, N. A. Suvorova, M. Jain, D. M. Feldmann, P. C. Dowden, R. F. DePaula, and Q. X. Jia, *Appl. Phys. Lett.* **92**, 102113 (2008).
- ²⁵I. B. Misirlioglu, M. B. Okatan, and S. P. Alpay, *J. Appl. Phys.* **108**, 034105 (2010).
- ²⁶L. Pintilie, V. Stancu, L. Trupina, and I. Pintilie, *Phys. Rev. B* **82**, 085319 (2010).
- ²⁷D. S. Shang, L. D. Chen, Q. Wang, W. Q. Zhang, Z. H. Wu, and X. M. Li, *Appl. Phys. Lett.* **89**, 172102 (2006).
- ²⁸R. Mazumder and A. Sen, *J. Alloys Compd.* **475**, 577 (2009).
- ²⁹S. M. Guo, Y. G. Zhao, C. M. Xiong, and P. L. Lang, *Appl. Phys. Lett.* **89**, 223506 (2006).
- ³⁰L. Pintilie, I. Vrejoiu, D. Hesse, G. Le Rhun, and M. Alexe, *Phys. Rev. B* **75**, 104103 (2007).
- ³¹L. Pintilie and M. Alexe, *J. Appl. Phys.* **98**, 123103 (2005).